Natural Hazards (2025) 121:19189–19215
https://doi.org/10.1007/s11069-025-07566-9

ORIGINAL PAPER

Changing hazards, exposure, and vulnerability in the conterminous United States 2020–2070

David N. Wear[1] · Travis Warziniack[2] · Claire O'Dea[3] · John Coulston[4]

Received: 30 January 2025 / Accepted: 1 August 2025 / Published online: 18 August 2025

Abstract
Natural resource systems are being reshaped by changes in climate, resulting in increased likelihoods of wildfire, water scarcity, and heat stress, along with other adverse outcomes that define potential harm across a broad spectrum of locales in the United States. We evaluate fifty-year, multiple scenario projections of resource hazards and population change from the USDA Forest Service 2020 Resources Planning Act Assessment to identify areas of concern based on hazard exposure and social vulnerability criteria and evaluate implications for climate adaptation and risk mitigation planning. We project how and where hazard exposure may change over the next fifty years and decompose changes into the portion driven by climate and population—both prove consequential. Water shortage projections show little change in spatial distribution but strong growth in the intensity of anticipated shortages. Wildfire projections show a structural change in pattern with emergent growth in wildfire extent in the southeastern US coincident with higher population densities and social vulnerability. High heat areas expand toward the north and east from the Southwest. Projections also show substantial growth in areas affected by two or more hazards and highlight where hazards correspond with high exposure and/or high vulnerability. For all hazard categories and scenarios, at least 80% of the population exposed to high hazard is in either a high vulnerability or high exposure county. Results highlight how management strategies would differ between those focused on mitigating the biophysical hazard alone and those that focus on mitigating exposure or vulnerability criteria.

Keywords Hazard exposure · Mitigation planning · Social vulnerability · Climate change

✉ David N. Wear
wear@rff.org

[1] Resources for the Future, Washington, DC, USA

[2] USDA Forest Service, Rocky Mountain Research Station, Fort Collins, CO, USA

[3] USDA Forest Service, Washington, DC, USA

[4] USDA Forest Service, Southern Research Station, Blacksburg, VA, USA

1 Introduction

Climate change portends widespread alteration of natural resource systems (USGCRP 2018) with complex consequences for human well-being and, in places, needs for both mitigation and adaptation. Increased likelihood of water scarcity (Heidari et al. 2021), wildfire (Westerling et al. 2006; Barbero et al. 2015; Burke et al. 2021), and heat stress (Chen et al. 2020; Schwingshackl et al. 2021; Yin et al. 2023), along with other adverse outcomes such as extreme weather (Bouwer 2013) and sea-level rise (Brown et al. 2021; Jevrejeva et al. 2023) define potential harm across a broad spectrum of locales in the United States. Because they are linked to common climate futures, these hazards are interrelated and can define compounding impacts. The risk of adverse outcomes arises from the intersection of biophysical hazards with the exposure of population and property in specific places and the vulnerability of exposed populations. The objective of this study is to use fifty-year projections of resource hazards and population change to identify areas of current and future concern and to evaluate implications for climate adaptation and risk mitigation planning.

Risk assessment provides the conceptual frame for our analysis where the risk of adverse outcomes or harm results from the interaction of biophysical hazards with the exposure of populations and property and the vulnerability of exposed populations. Monetary damage functions are unavailable for specific hazards, so we identify where projected hazards could co-occur with high exposure areas and/or highly vulnerable populations. A growing body of research addresses the correspondence of individual hazards and vulnerable communities (e.g., for water shortages (Saia et al. 2020; Sanchez et al. 2023) or for wildfire (Gaither et al. 2011). Some recent studies examine at a conceptual level how multiple hazards might interact (Tilloy et al. 2019; Drakes and Tate 2022), and mainly focused on biophysical interactions rather than human costs. We extend this literature by examining long run (fifty year) projections of multiple hazards—water shortage, wildfire, and heat stress—coupled with associated projections of exposed human populations and current measures of social vulnerability.

The USDA Forest Service 2020 Forests and Rangeland Renewable Resources Planning Act (RPA) Assessment (USDA Forest Service 2023) provides the hazard and population projections. Conducted every ten years since 1980 to examine whether renewable resources can continue to meet the needs of the American public, the RPA Assessment provides harmonized fifty-year projections of climate, economic factors, and natural resource supplies, demands, and conditions in the United States, including water and forest resources, across a common set of scenarios defined by downscaled climate futures (Representative Concentration Pathways or RCPs coupled with multiple General Circulation Models or GCMs (Joyce and Coulson 2020) and downscaled social conditions (Shared Socioeconomic Pathways or SSPs) (Langner et al. 2020; O'Dea et al. 2023). We use RPA Assessment projections of water shortage (Warziniack et al. 2023) and wildfire extent (Coulston et al. 2023a; Costanza et al. 2023) coupled with temperature projections from the GCMs used in the RPA Assessment (O'Dea et al. 2023; Langner et al. 2020) and intersect these with RPA projections of exposed populations (Wear and Prestemon 2019). While many hazards could be examined in this way, we only compared hazards from the 2020 RPA Assessment to ensure all projections were based on the same future scenarios. While the RPA Assessment projects more than just these hazards, these selections are frequently discussed in the literature as relevant to adaptation and mitigation planning and therefore this analysis provides a useful initial examination of the different ways that communities experience risk from hazards. Absent a practical means to project how vulnerability would evolve, we apply the Center for Disease Control's Social Vulnerability Index (SVI) for 2020 (Flanagan et al. 2018) to examine the intersection of future hazards/populations with current measures of social vulnerability—i.e., where current vulnerable communities will likely face high hazards in the future. Multiple scenarios of future conditions allow us to gauge the range and variability of the projections.

We project how and where exposure may change over the next fifty years and decompose change into the portion defined by climate driven changes in hazard occurrence and the portion driven by socioeconomic/population changes. We compare the implications of prioritizing mitigation activities based on areas with the greatest exposure to multiple hazards, measured here as population density, with prioritizing based on present-day social vulnerability. By examining where priorities based on these two criteria are divergent or complementary, these projections provide a tool for exploring implications of risk mitigation activity placement. They provide a foundation for cost benefit analysis of risk mitigation investments and could be used to prioritize investments that anticipate how and where risk mitigation may evolve in the future.

Federal investments are often guided by regulations that combine efficiency and equity criteria, for example national forest planning as guided by the National Forest Management Act (P.L. 94–588) seeks to maximize returns to the American public while stabilizing local communities. Economists have long recognized that efficiency and equity are foundational but distinct rationales for public sector interventions and imply tradeoffs (Atkinson and Stiglitz 1980). We identify and compare priority areas for hazard mitigation based on total expected harm defined as the exposure of people to harm (an efficiency measure) with priority areas based on vulnerability of exposed communities (an equity measure). We examine where these areas diverge and discuss the challenges faced by federal and state agencies seeking to balance provision of maximum benefits and distribute benefits equitably.

Our results –specifically the comparison of locations of future hazard, future hazard exposure, and current vulnerability—demonstrate where selecting priority areas focused on mitigating biophysical hazard alone diverges from selecting areas that focus on mitigating exposure or vulnerability criteria. They also highlight that these priority areas are expected to change over time, especially in response to regional shifts in wildfire risk. Where these areas are consistent using both exposure and vulnerability criteria, choices are less ambiguous. Where these priority areas diverge, allocating limited resources to try to manage for both efficiency and equity goals becomes increasingly difficult. Our study and others are challenged by fundamental measurement and modelling limitations—including the measures of vulnerability and exposure and a lack of explicit damage functions. Still, results highlight that hazard and risk are likely to change substantially in coming decades, greatly expanding the amount and severity of hazard and exposed population and altering the spatial pattern of exposure and vulnerability.

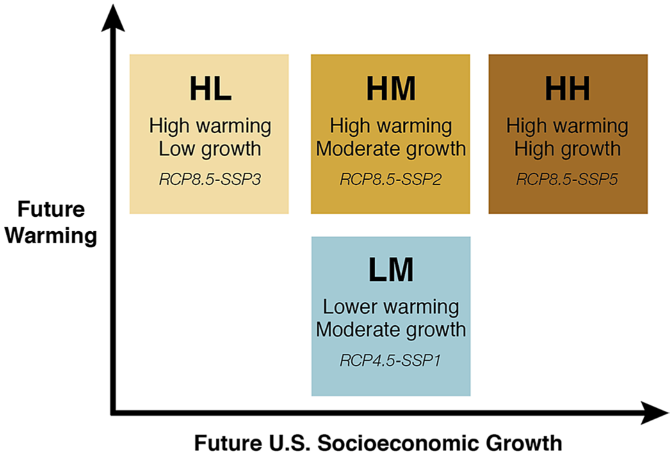

Fig. 1 RPA scenarios as defined by the intersection of Representative Concentration Pathways and Shared Socioeconomic Pathways

2 Methods

We evaluate the future effects of multiple hazards on communities arrayed by measures of exposure and social vulnerability. Hazard probabilities derive from stochastic simulations of hydrology/water uses and forest dynamics developed for the 2020 RPA Assessment and underlying climate models (Costanza et al. 2023; Coulston et al. 2023a; Warziniack et al. 2023). Absent specific damage functions for these hazards, we approximate exposure using projections of populations and approximate vulnerability with the Social Vulnerability Index or SVI for 2020 (Flanagan et al. 2018) a measure of relative social vulnerability provided by the Centers for Disease Control (CDC). SVI has been similarly used to evaluate vulnerability to water scarcity and/or flooding (Saia et al. 2020; Sanchez et al. 2023) and fire hazards (Modaresi Rad et al. 2023) and is readily decomposed to examine component drivers of vulnerability.

The RPA Assessment's projections address a common set of scenarios defined by climate futures driven by Representative Concentration Pathways (RCP4.5 and RCP8.5) paired with socioeconomic futures defined by Shared Socioeconomic Pathways (O'Dea et al. 2023). RPA models apply downscaled climate futures from several General Circulation Models or GCMs (Joyce and Coulson 2020) that can be reaggregated as required—e.g., to HUC based watersheds or to counties—and downscaled SSP futures of income and population using an empirical model based on economic growth theory (Wear and Prestemon 2019) to project changes at the county level. We use three of the four RPA scenarios shown in Fig. 1: 1) RCP4.5 (lower radiative forcing) combined with SSP1 (moderate domestic economic growth) and labeled LM, 2), RCP8.5 (high radiative forcing) combined with SSP3 (low domestic economic growth) and labeled HL, and 3), RCP8.5 (high radiative forcing) combined with SSP5 (high domestic economic growth) and labeled HH.[1] Taken together,

[1] We do not include the remaining HM scenario with high radiative forcing and moderate domestic economic growth, because its results are bracketed by HL and HH.

scenarios bracket a plausible range of future conditions organized by the familiar form of global climate change analysis.[2]

We use fifty-year projections, the temporal extent of the RPA, summarized at the county scale, a grain that is consistent with long-term strategic land management problems, where agencies manage broad landscapes with effects that span multiple communities that have a broad zone of influence. While field level planning requires more highly resolved spatial analysis, the county grain allows a high-level assessment useful for setting priorities and designing broad strategies. Projections of water shortage (Warziniack et al. 2023), fire frequency (Constanza et al. 2023), temperature (Joyce and Coulson 2020), and population (Wear and Prestemon 2019) all originate from the 2020 RPA Assessment (USDA 2023). We note that models have varying starting years (as early as 2015) and adopt that Assessment's reconciliation of disparate time steps but point out that most resource conditions evaluated here evolve slowly so that this reconciliation should not introduce bias to the analysis.

2.1 Water shortage projections

Water scarcity and drought has become more common and severe in the western United States and vulnerable populations are disproportionately exposed to their impacts (Sanchez et al. 2023). We apply projections of water shortage from the Water Resources Chapter of the 2020 RPA Assessment (Warziniack et al. 2023). Water shortage is the result of projections for both water demand and water supply (Heidari et al. 2021) and occurs when demands for water are partially or fully unmet. The model is run at monthly timesteps and accounts for instream flow requirements, reservoir storage, and trans-basin transfers of water.

Following Sanchez et al. (2023), our measure of shortage is defined as shortages of at least 12 months in duration expected to occur approximately once in a 50-year period. Projections are generated for HUC4 watersheds that we rescale to counties as the area-weighted average of watershed conditions within each county after joining HUC4 and county polygons. We evaluate changes in shortage conditions for future scenarios by comparing baseline or current conditions (1986 to 2015) with projected future conditions. We then assign counties a shortage category (from low to high). Projections define the intensities of shortage events (million cubic meters per month) which are dominated by zeros at the county level. We assign the lowest shortage category to county values of less than or equal to zero. We then partition the remaining counties with positive shortage values by terciles (medium low, medium high, high) for the LM scenario in 2020 and apply the same breaks to other scenarios and projection years to allow for comparison across scenarios and time. This defines a simulated base case from which future changes are gauged.

2.2 Fire frequency projections

In the western United States, changes in forest vegetation combined with adverse weather conditions have resulted in increasingly intense wildfires with growing costs from lost lives, health impacts, property, and community infrastructure. Across the United States the annual

[2] In this way, the RPA Assessment is consistent with the structure of the IPCC (IPCC 2022) and US climate change assessments (USGCRP 2018) and provides key inputs to the latter.

cost burden is estimated to be between \$394 billion and \$893 billion.[3] Social conditions, notably the distribution of wildland-urban interface areas strongly affect these costs and vulnerable populations may be more heavily exposed to wildfire (Rad et al. 2023). RPA projections of wildfire occurrence account for the dynamics of forest conditions, land use, and climate change.

We apply wildfire area projections from the Forest Resources chapter of the RPA Assessment. The Forest Dynamics Model, or FDM (Coulston et al. 2023a, b) projects future forest inventories for all regions of the United States by simultaneously accounting for forest growth dynamics, land use changes, timber production, and disturbances including wildfire. Forest dynamics are modeled at the inventory plot level (each plot represents 6,000 acres in an area frame sampling protocol) using stochastic event models for wildfire, timber harvesting, and other disturbances that are influenced by scenario inputs. Based on simulated events, individual plot conditions are assigned using stochastic imputation using historical records from > 150,000 US Forest Service forest inventory plots (Westfall et al. 2022) for multiple realizations for each scenario. Socioeconomic and climate variables that define scenarios also affect future land use and land use changes (Riitters et al. 2023) which shift the area represented by each plot within the future inventory. That is, each scenario includes an exogenous projection of population and personal income that alters the demands for land in all uses and therefore results in land use changes. For the scenarios evaluated here, these projected changes in land use lead to small net declines in forestland (Riitters et al. 2023 for land use projections by scenario).

Projected wildfire occurrence is modeled as a discrete event at the plot level as influenced by projected climate conditions but also indirectly through projected changes in forest conditions (Costanza et al. 2023). Changes in wildfire patterns over time can therefore reflect how wildfire along with growth, disturbance, harvesting and land use changes alters future forest fuels. We define the projected frequency of wildfire measured as the areal portion of total land burned within a county over a decadal time step. We evaluate changes in fire frequency between a baseline case (2020–2030) and values projected for 2060–2070. FDM projections of fire frequency for each scenario result from Monte Carlo simulations averaged across five climate models. We assign risk categories (low, medium low, medium high, and high) by partitioning counties by quartile for the LM scenario in 2020–2030 and then use the breaks to apply the same categories to the other scenarios and years (this defines a simulated base case from which departures are gauged). Our analysis implicitly focuses on fire hazards occurring within a county and does not address the transfer of smoke to downwind counties.

2.3 Temperature projections

Heat stress defines a direct impact of climate change for human communities. As temperatures or other heat stress indicators (such as wet bulb temperature and NOAA heat index) exceed health-related thresholds more frequently, human health, mortality, and economic activity are negatively impacted (Schwingshackl et al. 2021; Yin et al. 2023). The realized harm of heat stress is strongly linked to certain aspects of social vulnerability. For example,

[3] These cost estimates are from the US Congress Joint Economic Committee, dated October 2023: https://www.jec.senate.gov/public/_cache/files/9220abde-7b60-4d05-ba0a-8cc20df44c7d/jec-report-on-total-costs-of-wildfires.pdf.

elderly populations are most likely to suffer increased mortality and morbidity, and these impacts are likely to be amplified as U.S. populations age (Chen et al. 2020). The ability of local populations to adapt to heat stress is also associated with income (for example, as it affects access to air conditioning).

While we project specific hazards for fire and water scarcity, we use a measure of temperature change as a proxy for potential harm from added heat stress—harm in the form of variables such as human health impacts and loss of income. Climate projections are variable within years and across locations with varying implications for especially damaging heat waves (Mukherjee et al. 2021). Rather than directly model heat stress events, which was beyond the scope of the 2020 RPA Assessment, we use a climate analog approach with a proxy for annual temperature regime, including heat stress, defined by the average maximum daily temperatures for June, July, and August, further averaged across the GCMs used for each scenario. We average maximum temperatures within each county on a decadal time step across GCMs and then compare averages between a baseline (2020) and projections for 2070. We assign four heat categories as follows: high is >37.8 C (>100 F), medium-high is 35–37.8 C (95–100 F), medium-low is 29.4–35 C (85–90), and low is all temperatures below 29.4 C (85 F). These categories derive from an analysis of most recent temperature profiles of places in the U.S. Our scheme defines high heat category in the base period consistent with temperatures in the ten hottest counties in the US—in an area at the intersection of Arizona, California, and Mexico, and in far southern Texas (2020). Medium high temperatures are associated with counties in western and central Texas, southern New Mexico and Arizona. Projections therefore define future areas of heat consistent with these locational analogs.

2.4 Exposed populations

RPA Assessment projections of population define changes in exposure for all scenarios. They were derived from national level SSP projections for the US from the IIASA Integrated Assessment Model (Crespo Cuaresma 2017) and downscaled to the county level using methods described in Wear and Prestemon (2019)—2020 population estimates are shown in Fig. 2. They jointly downscale income and population projections to reflect wage driven migration and income convergence consistent with historical patterns of change, but do not account for how climate might affect these variables. SSP3, the low domestic growth scenario, shows moderate population growth until 2040 and then a return to current population numbers by 2070. For SSP3, population declines in much of the northeast with growth around some population centers in the southeast and southwest. For SSP1, population grows by about 40% between 2015 and 2070 with growth around most existing population centers but with higher rates of growth in the southern and western regions. The same pattern holds for SSP5, the high growth pathway, but population grows by 80% over this period. We also considered using population totals by county to gauge exposure, but settled on using the population density as the measure of population exposure because the county size varied by three orders of magnitude from a minimum of 24 sq mi to a maximum of 20.1 thousand sq mi.

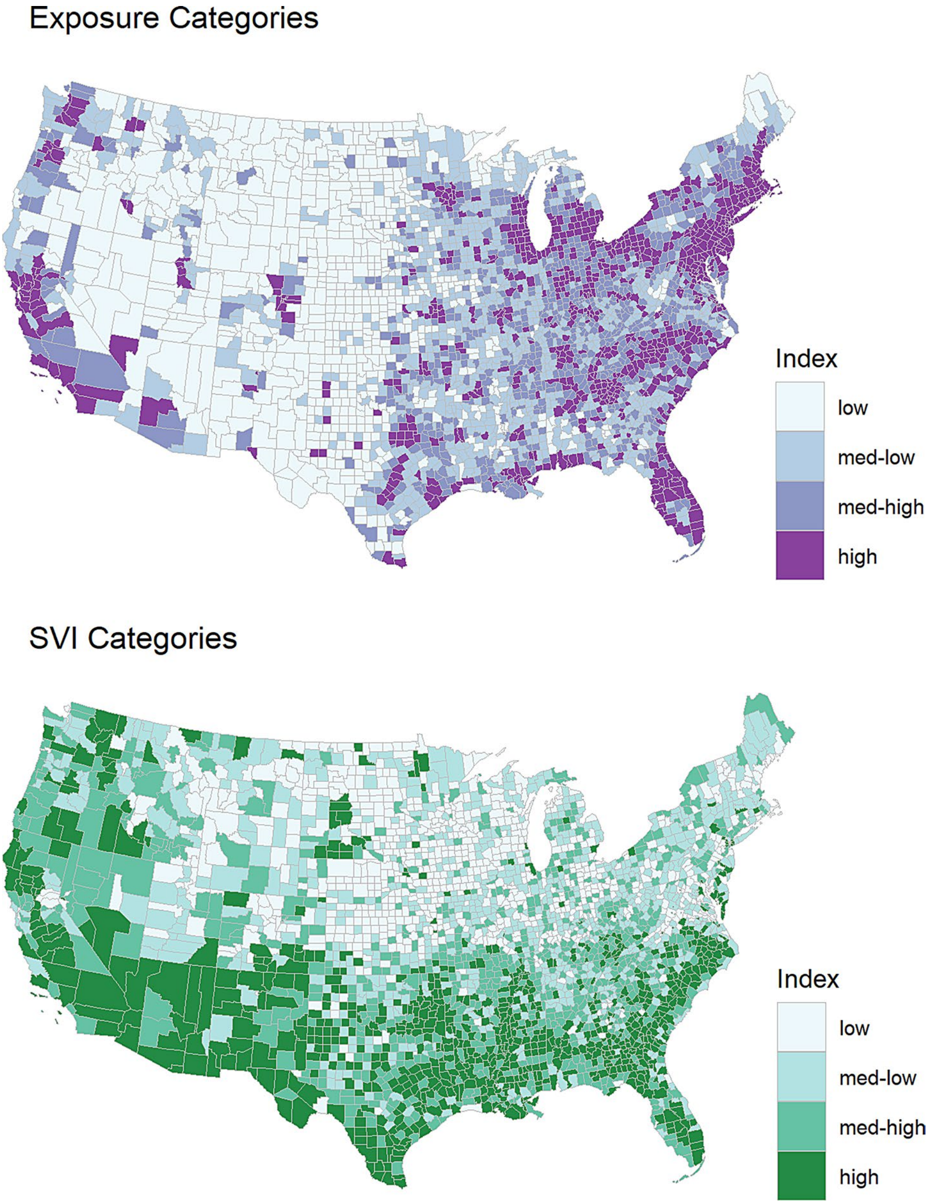

Fig. 2 Maps of an exposure index (2020 population density) and a social vulnerability index (2020 CDC-SVI) with counties divided into value quartiles (low, medium-low, medium-high, and high)

2.5 Social vulnerability

Social vulnerability cannot be directly observed, and various indices have been used as proxies. An index of social vulnerability accounts for how various factors contribute to individuals' and a community's ability to influence its future and/or recover from adverse events such as natural disasters (Cutter et al. 2003; Cutter and Finch 2008; Flanagan et al. 2011, 2018) using indicators of health access and mobility (e.g., the size of elderly and disabled populations); dimensions of local infrastructure (e.g., access to transportation or the quality of the housing stock); and determinants of historical marginalization including income, poverty rates, and racial/ethnic minority status. While regularly deployed, these broad measures of vulnerability may not be best for assessing the impacts of any specific hazard (Spielman et al. 2020). Ideally, measures of vulnerability would be constructed to address vulnerabilities to specific hazards (Drakes and Tate 2022) and would themselves be projected. However, given the broad scope of our study, with multiple hazards, multiple scenarios, and a national focus, we consider a general index of vulnerability the only practical approach.

Federal agencies have used various indices of vulnerability.[4] We used the SVI from the Centers for Disease Control (Flanagan et al. 2011, 2018) to rank the relative vulnerability of communities because it accounts for several dimensions using a straightforward analytical technique applied to widely available data. Unlike some other measures, it provides an ordinal ranking of vulnerability that does not embed climate or environmental hazard futures, which we address separately. The SVI is constructed and available at both Census tract and county scales. A drawback of using counties is the potential for amplifying the ecological fallacy when compared to finer grain measures—i.e., the fallacy that the ranking for the county applies to all communities it contains. Given our focus on broad scale hazards (e.g., not localized measures such as flooding), analysis at the county level provides useful information for broad scale strategic planning, but not necessarily for site level tactical analysis. These methods could be readily extended to finer grains, for example to census tracts if population projections could be downscaled to this level of resolution.

The SVI derives from conditions organized by four themes: socioeconomic status, household composition, minority status, and housing and transportation conditions, as well as an overall aggregate measure of vulnerability (Fig. 2). Following the CDC methodology, the aggregate vulnerability score is determined by summing the scores from all domains and dividing counties by quartile values: the highest 25% are assigned a "high" SVI rating, the lowest 25% a "low" rating and so on. The Midwest and northeast have comparatively low numbers of high SVI counties, while the concentration is much higher in the southeastern and southwestern regions and somewhat intermediate in the Pacific Northwest. The intermix of high and low vulnerability across the US highlights the spatial diversity of socioeconomic conditions. For example, in the Southeast, high social vulnerability for counties removed from the Coast—in the upper Coastal Plain, the lower Mississippi Alluvial Plain, and southern Appalachians—are largely linked to socioeconomic status and minority status (Fig. 2). High vulnerability counties in the Pacific Northwest generally arise from the household composition and minority status variables.

2.6 Risk analysis

Our risk matrix approach examines how hazards could affect communities in the future by comparing categories of hazard with categories of exposure or vulnerability as shown in

[4] The Centers for Disease Control considers community attributes in their programs addressing exposure to toxins using a Social Vulnerability Index (SVI) that accounts for multiple sources of vulnerability to rank communities (Flanagan et al. 2011), while the Federal Emergency Management Agency uses a different index of vulnerability (Cutter et al. 2003) for risk mapping and targeting investments in disaster mitigation.

Fig. 3—population or SVI is arrayed from low to high along the x axis and hazard likelihood is arrayed from low to high along the y axis. The bottom row describes conditions where expected hazard is minimal. The left column describes conditions where exposure or vulnerability is minimal. The upper right-hand corner of Fig. 3a and b defines a condition where both hazard and exposure or vulnerability are both at their highest levels consistent with the highest potential for harm.

The definitions of exposure, vulnerability, and hazard categories are highly influential for this type of analysis. Following standard practice, we array counties by SVI score quartiles to define the column ranks. We follow the same scheme for population density, our exposure measure. For example, in Fig. 3b, the 25% of counties with the highest SVI are in the right column with the deepest color green. The approach for assigning hazard categories (y axis) is not based on quartiles or equal shares as explained above—one reason is that the distributions of hazard are heavily skewed to the right, and another is that we seek some link to actual harm/damage thresholds. Ideally, we would identify thresholds that link the level of hazard exposure to a direct measure of physical or economic damage. But these relationships are not known, especially at this scale of analysis, so we develop separate qualitative means to define low to high impact classes. For temperature, we use a spatial analogue approach based on baseline temperatures that can map hazard to potential harm. Water shortage and wildfire hazard projections involve multiple resource dynamics (e.g., water demands, vegetation growth and mortality) that make construction of a spatial analogue impractical. We therefore use a proportional split of hazard projections to define hazard categories as described above.

We apply the risk matrix approach to identify the intersection of individual hazard likelihood with high exposure and high vulnerability counties. We start by mapping risks by categories. We then intersect these results to define where risks are co-occurring and potentially compounding. We then use the risk matrix to define focal areas based on exposure and on vulnerability and their spatial arrangement. As a final step we decompose changes in exposure and vulnerable populations into portions represented by climate change and population change over the assessment period. Define, for example, the total population exposed to a high hazard condition as $H * pop$, where pop is a k x1 vector of population counts for k counties and H is a 1 x k vector of 1's and 0's indicating presence or absence of high hazard respectively. The change in the population exposed to high hazard is approximated using the product rule for a discrete difference equation:

$$\Delta\ (H * pop) = H_{t+1} * pop_{t+1} - H_t * pop_t = \Delta\, H * pop_t + \Delta\, pop * H_{t+1}$$

Where Δ indicates difference over the evaluation period (t, t+1) so the first term on the right-hand side of the equation is the effect of changes in hazard attributable to climate change and

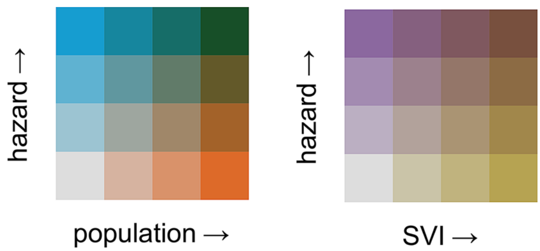

Fig. 3 Risk matrix comparing the population exposed or the social vulnerability index (2020 CDC-SVI) with hazard category. Axes are defined by increasing levels of hazard (y-axis) and either exposure or vulnerability (x-axis)

the second term is the effect of population growth on overall change in exposure. The same relationship is used to decompose the effects on vulnerable populations.

3 Results

3.1 Hazard projections

We report the area and populations exposed to hazards by category for the baseline period (2020–2030) and for projections for 2070 for the three scenarios: LM (RCP4.5-SSP1), HL (RCP8.5-SSP3), and HH (RCP8.5- SSP5). We decompose change in populations exposed into two components: change in hazard category and change in population. We identify the portion of change in exposure that arises in high vulnerability counties.

Baseline water shortage (Fig. 4) shows moderate water shortage across most of the Great Plains from Nebraska to the Mexican border and from the Rockies to the Mississippi. Additionally in the West, moderate water shortage hazard occurs in southwestern and intermountain west desert areas, throughout California and into southern Oregon. In the East, moderate water shortage hazard is found in an area of Illinois/Indiana/Michigan centered on Chicago, southern Louisiana, and much of peninsular Florida into southeastern Georgia.

Water shortage projections to 2070 show little change in the overall locational pattern. All scenarios show some intensification of hazard within these areas with somewhat dissimilar patterns. For all scenarios, water shortage risk increases to the highest category in southwestern Texas, a large portion of New Mexico/Arizona, and southern Louisiana. For HH and HL based on RCP 8.5, the area of high hazard expands outward from baseline areas and emerges in southern Michigan. Parts of the Pacific US, mainly in California, are wetter or see little change in water yield under some of the climate projections so improvements in water use efficiency actually lead to reductions in the extent of water shortages.

High water shortage areas increase from no area in 2020 to 59 million hectares for LM, 87 MM ha for HL, and 88 MM ha for HH (Fig. 4a). Population growth accounts for 11% of the increasing exposure to high shortage for HL, the lowest population growth scenario, 53% of the increasing exposure for HH, the highest population growth scenario, and 40% of the increasing exposure for LM (Fig. 4b). The projected portion of exposed populations located in high social vulnerability counties ranges from 50% for HL to 80% for LM (Fig. 4b and c).

For wildfire, baseline hazard maps (Fig. 5d) show a clustering of high-risk areas in a few locations. In the West, this includes a large portion of the northern Rockies, an area in Washington along the Canadian border, and, most substantially a region stretching from the Klamath Mountains in southern Oregon, southward through the Sierra Mountains. In the East, areas of high risk are smaller and include an area in southeastern Missouri and some scattered counties from southeastern Georgia into Florida. Areas of medium high risk extend from and generally connect the areas of high risk in both the East and the West.

Wildfire hazard projected to 2070 shows intensification and spread of hazard from the baseline areas (Fig. 5d). The area of high hazard grows especially in the Klamath-Sierra subregion but also in the northern Rockies. Projections also show new areas of high hazard emerging in the southern Rockies in New Mexico, and a large area of medium-high hazard in the front range of Colorado. The most substantial change in fire pattern and magnitude,

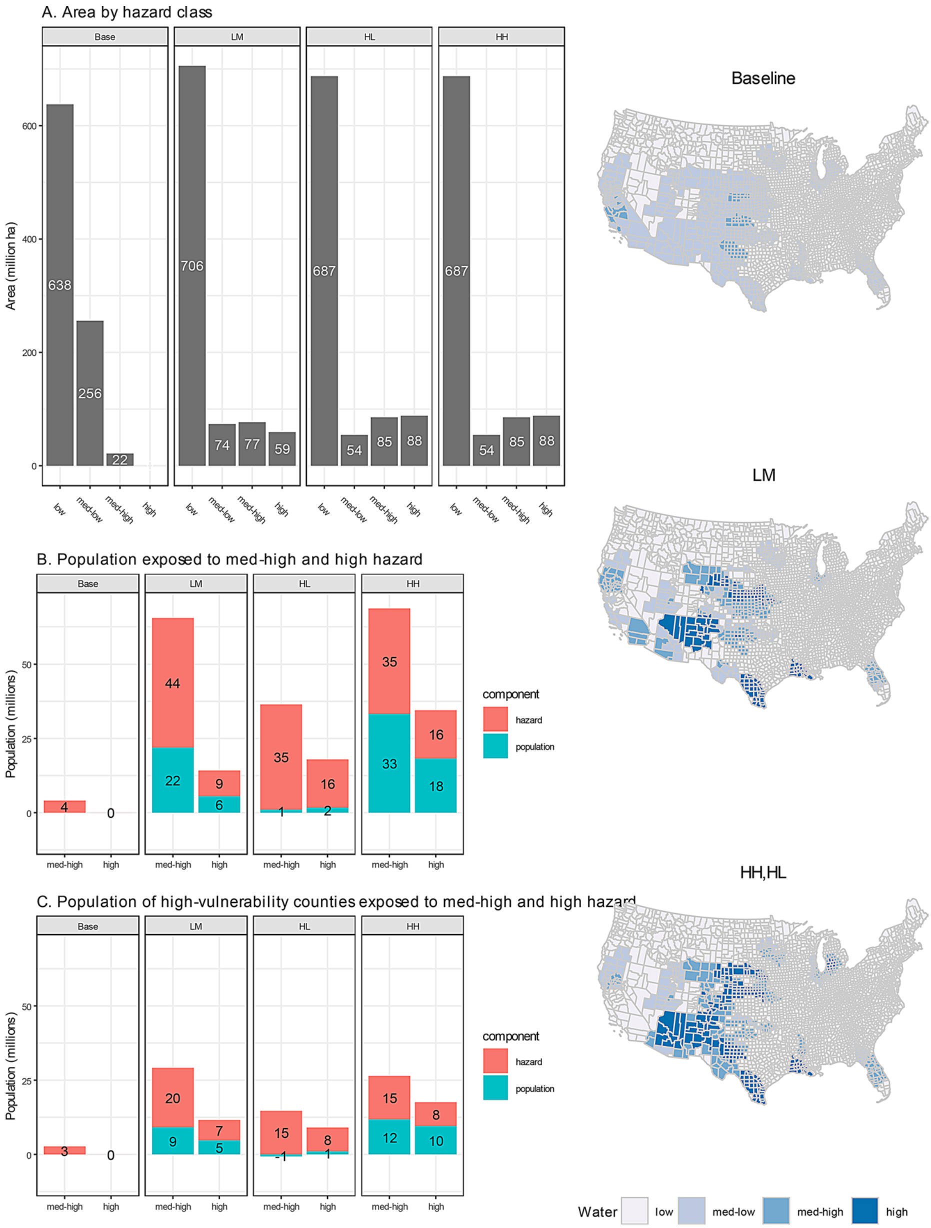

Fig. 4 Baseline and projected (2070) water shortage by hazard class and scenario with **A**) area by hazard class, **B**) exposed populations for medium-high and high classes, **C**) exposed populations in high vulnerability counties for medium-high and high classes, and D) county mappings. For water shortage, hazard projections do not vary between HH and HL scenarios. Three scenarios are evaluated: LM using RCP4.5 (lower radiative forcing) climate projections combined with SSP1 (moderate domestic economic growth), HL: using RCP8.5 (high radiative forcing) combined with SSP3 (low domestic economic growth), HH: RCP8.5 (high radiative forcing) combined with SSP5 (high domestic economic growth)

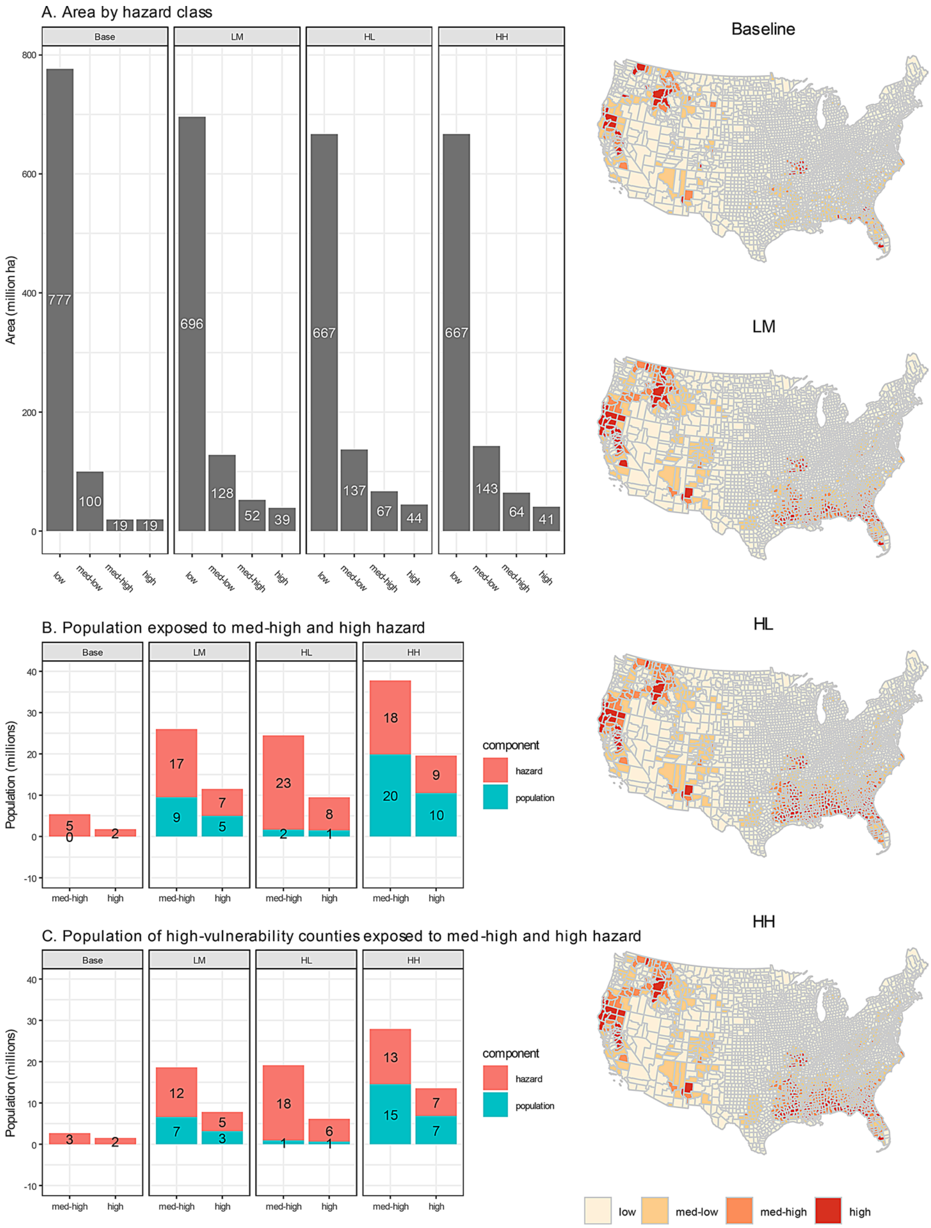

Fig. 5 Baseline and projected (2070) wildfire hazards by hazard class and scenario with **A**) area by hazard class, **B**) exposed populations for medium-high and high classes, **C**) exposed populations in high vulnerability counties for medium-high and high classes, and **D**) county mappings. Three scenarios are evaluated: LM using RCP4.5 (lower radiative forcing) climate projections combined with SSP1 (moderate domestic economic growth), HL: using RCP8.5 (high radiative forcing) combined with SSP3 (low domestic economic growth), HH: RCP8.5 (high radiative forcing) combined with SSP5 (high domestic economic growth)

however, arises in the southeastern United States, with high-hazard areas emerging in both the upper and lower Gulf of Mexico Coastal Plain, from East Texas to Florida and southern Georgia for all three scenarios. LM, which is based on climate futures from RCP4.5, shows more growth in western fire hazard while HL and HH, based on climate futures from RCP8.5, shows more growth in fire hazard in the Southeast and less in the West.

Overall, the area exposed to high wildfire hazard roughly doubles between 2020 and 2070 for all scenarios (from 19 million hectares (MM ha) to 39-44MM ha; Fig. 5a) while the area of medium high hazard roughly triples (from 19 MM ha to 52–64 MM ha). The total population exposed to high wildfire hazard grows at a much higher rate and varies more across scenarios (Fig. 5b)—from 2 million people (MM P) in 2020 to 9 MM P for HL, 11 MM P for LM, and 20 MM P for HH (10x), consistent with the population growth ordering of the three scenarios. A similar pattern holds across scenarios for exposure to medium high wildfire hazard.

For scenarios HH and LM, between 45 and 55% of growth in wildfire exposure is due to population growth and the remainder is due to changes in area of hazard (Fig. 5b). For HL, the scenario with the lowest rate of population growth, only 11% of growth in wildfire exposure is due to population growth. The portion of exposed populations located in counties with high social vulnerability is projected to be much more consistent across scenarios: from 70% for HH to 72% for LM, to 77% for HL (Fig. 5b and c).

Baseline areas of high heat are found along the southern borders of Arizona and California and in a small number of counties in West Texas, mainly along the US-Mexico border south of Del Rio (Fig. 6d). Areas of medium-high heat are found in much of southern Arizona and the remainder of Texas. Under LM, the area of high heat triples from 6 MM ha to 20 MM ha. Under HL and HH (both based on the same RCP8.5 climate projections), the area of high heat grows more than twenty-fold to 126 MM ha. High heat areas expand east and north from their baseline loci through most of Texas and into Oklahoma, Louisiana, Mississippi, and Arkansas and also emerge in much of the upper coastal plain of Georgia and South Carolina by 2070. The area of medium-high heat, consistent with baseline conditions in central Texas, expands across much of the Southeast (areas south of a line from Oklahoma to North Carolina) and in Kansas and Missouri.

The population exposed to high heat grows more substantially than area, from 1 MM P in the baseline to 14 MM P under LM and to 49- and 92-MM P for the HL and HH scenarios respectively. The share of exposure growth attributable to population growth ranges from 11% for HL to 43% for LM to 52% for HH (Fig. 6b). For the baseline and LM, nearly all exposed populations are in high vulnerability counties (Fig. 6b and c). For HL and HH 55% and 56% of exposed populations are in high vulnerability counties respectively.

Patterns of baseline and projected hazard are generally distinct between wildfire, water shortages, and heat stress but some areas of overlap arise. If we reduce risk categories to binary classes (presence or absence) these overlapping areas are easier to discern. Evaluating medium high and high hazard categories (medium threshold) yields the first column in Fig. 7 for the baseline and projections for LM, HL and HH scenarios. The color brown indicates where all three hazards cooccur. No three-way intersections arise in the baseline. All three future scenarios show some brown counties in southern Louisiana and further up the Mississippi Delta and in an area from central to northern peninsular Florida. Two-way intersections arise in several areas: wildfire and water shortages cooccur in areas of New Mexico and Arizona, and an area from the northern Central Valley to the Cascades in northern Cali-

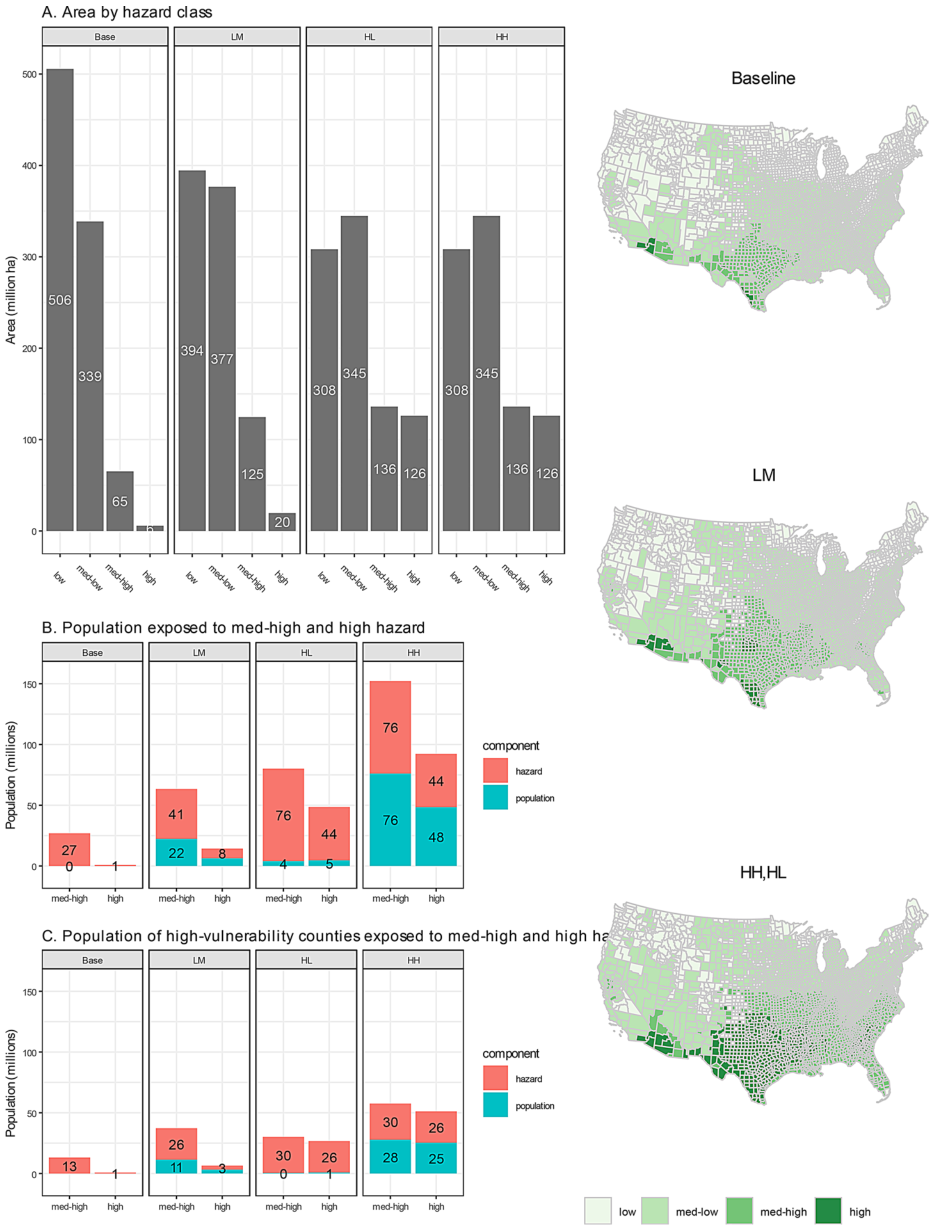

Fig. 6 Baseline and projected (2070) heat by hazard class and scenario with **A**) area by hazard class, **B**) exposed populations for medium-high and high classes, **C**) exposed populations in high vulnerability counties for medium-high and high classes, and **D**) county mappings. For heat, hazard projections do not vary between HH and HL scenarios. Three scenarios are evaluated: LM using RCP4.5 (lower radiative forcing) climate projections combined with SSP1 (moderate domestic economic growth), HL: using RCP8.5 (high radiative forcing) combined with SSP3 (low domestic economic growth), HH: RCP8.5 (high radiative forcing) combined with SSP5 (high domestic economic growth)

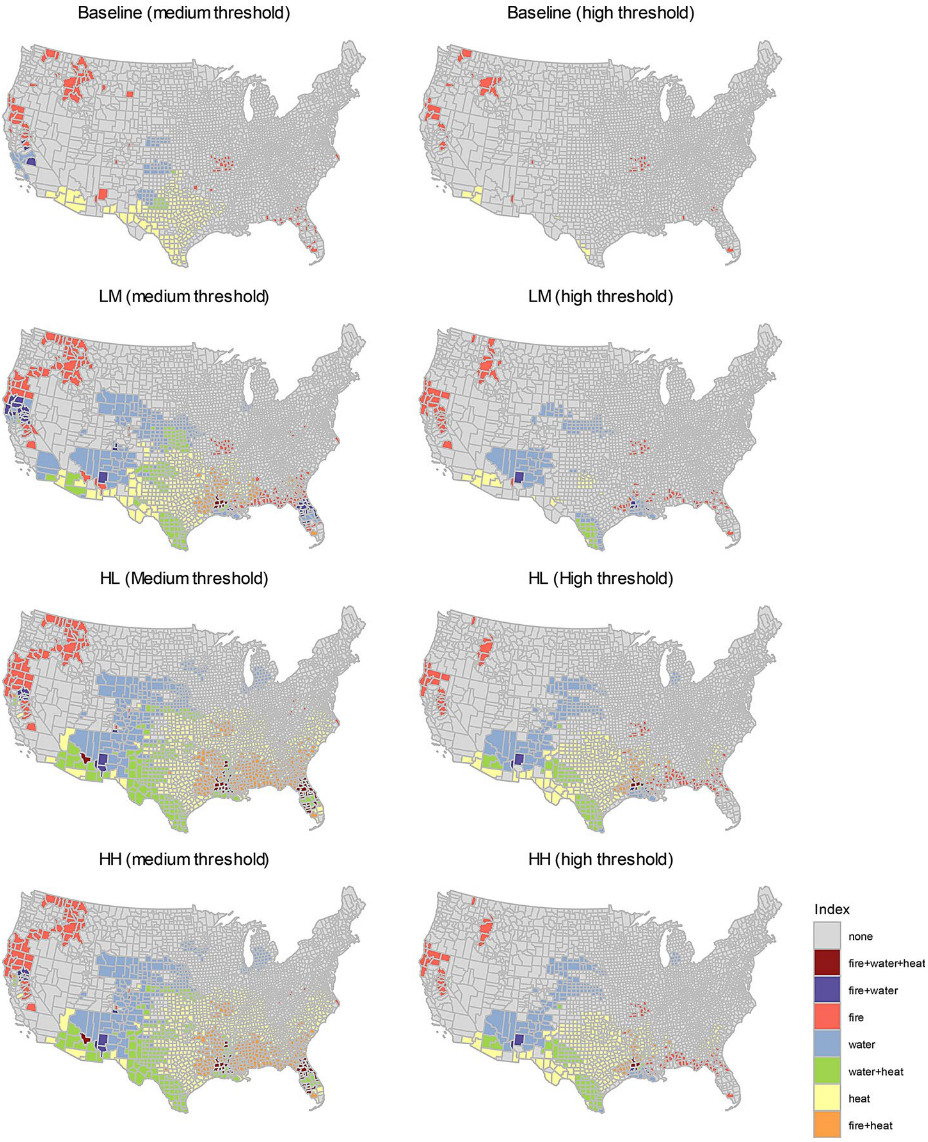

Fig. 7 Overlay of hazard locations for the baseline in 2020 and for projections to 2070 for scenarios LM, HL, and HH. The left column, labeled "medium threshold," maps counties with either Medium-high or High categories of hazard. The right column, labeled "High threshold" maps counties with only High categories of hazard

fornia. High heat and water shortage cooccur in western Texas and through areas of New Mexico and Arizona, in portions of Oklahoma, and in an area within the lower Mississippi Alluvial Valley. The intersection of high heat and wildfire defines the greatest area of co-occurring hazards, arising strictly within the Southeast, across the Atlantic and Gulf Coastal Plain region from east Texas to the Atlantic Coast. The extent of co-occurrence varies across scenarios—HL and HH generally have greater areas of co-occurrence, but the area of co-occurring wildfire and water shortage in California is greater under the LM scenario.

Using a high hazard threshold (right column in Fig. 7) greatly reduces the area of overlapping hazards. All three hazards overlap at the at the high threshold for only a small number of counties in southern Louisiana. Fire and water shortage co-occur only in an area at the border of New Mexico and Texas. Water shortage and heat co-occur at high levels in smaller portions of central Arizona and southern and south-central Texas. Heat and fire hazards co-occur at high levels in Louisiana and northward in the Mississippi alluvial valley north to Tennessee.

3.2 Risk analysis

Mapping hazards and their co-occurrence summarizes the information contained in the RPA simulation models as driven by climate/socioeconomic scenario data. But biophysical measures alone do not describe potential harm to humans and communities. For this we intersect hazard categories with categories of exposure and vulnerability. The intersection of the three hazards and exposure (Fig. 8) show distinct profiles for wildfire, water shortage, and heat stress.

For the baseline, high wildfire hazards co-occur with high exposure in only two counties in the Southeast. Projections of wildfire hazard indicate some growth in high hazard/high exposure counties in the Sierra Mountains (the mountain range that spans central California) and more so in the lower Coastal Plain in the Southeast. The intersection between high water shortage hazard and high exposure arises in southwestern Arizona, southern Texas, and southeastern Louisiana. In addition, areas around Lake Michigan (northern Illinois and southwestern Michigan) show a concurrence of high water shortage and high exposure in 2070 for all scenarios. High exposure areas for heat stress are projected to expand in southern Texas, with medium-high exposure across most urban areas of west Texas, and in southern peninsular Florida.

High vulnerability as proxied by SVI describes where community structure indicates increased potential for individual/community harm (Fig. 9). For baseline conditions, high wildfire hazard and high vulnerability co-occur in three areas: northern Washington along the border with Canada, northern California, southeastern Missouri, and in a few (four) scattered counties in the Southeast. Consistent with growth in fire hazard described above, the area of intersection grows substantially to 2070 for all scenarios, especially in northern California/southern Oregon but also across an emergent and large area of high hazard/high vulnerability in the southeastern coastal plain.

Substantial growth in the projected area of water shortage to 2070 leads to intersections of high water shortage hazard with high SVI in three areas: an area of Arizona and New Mexico (this area is especially large under the HH scenario where it grows into southern Colorado), southern Texas along the border with Mexico south of Del Rio, and a large portion of the lower Mississippi Alluvial Plain in Louisiana and Mississippi.

For heat, baseline conditions show three small clusters of high vulnerability/high hazard intersections between southwestern Arizona and far southern Texas. For the LM scenario, growth in co-occurrence expands somewhat from the two baseline locations in Texas. For the HH scenario, the intersection expands substantially to the north from the Texas locations but also emerges in much of southern Florida.

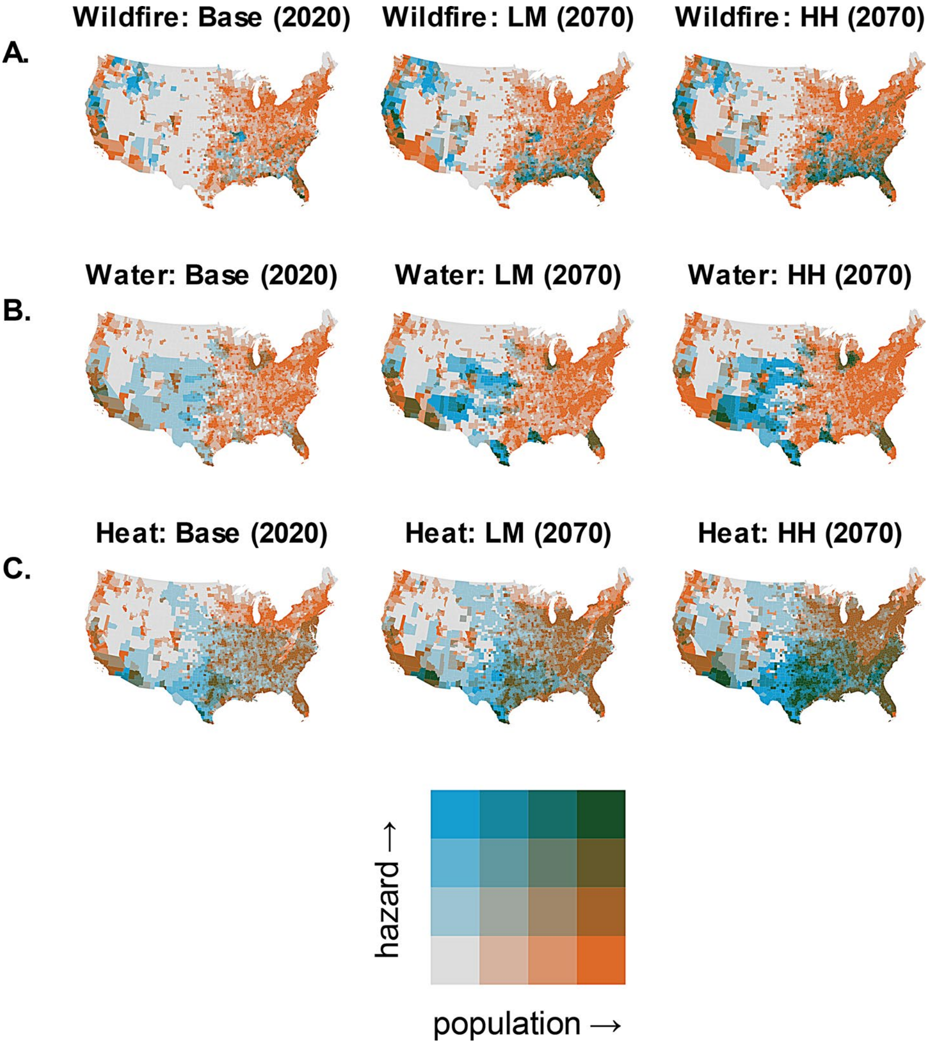

Fig. 8 Bivariate mapping of risk and population density, a measure of exposure, for: **A**. wildfire, **B**. water shortage, and **C**. heat stress. Columns, from left to right, contain estimates for base period (2020–2030) and for projections to 2070 for LM and HH scenarios. Both population density and risk are arrayed into three categories: low, medium-low, medium-high, and high using quartiles for population density and risk classification schemes described in the methods for hazard risk

We next intersect social vulnerability and exposure analyses to highlight areas of concern and where they co-occur. We define an area of concern as the intersection of medium-high or high hazard (medium threshold as defined above) with medium-high or high exposure and/or vulnerability categories (this defines the upper right quadrant of the bivariate classifications in Figs. 8 and 9). For wildfire, a highly complex landscape of potential wildfire harm already exists in northern California to southern Oregon with several counties with both high vulnerability and high exposure (Fig. 10). Another area of potential wildfire harm occurs in the northern Rocky Mountains (the mountainous areas of western Montana and

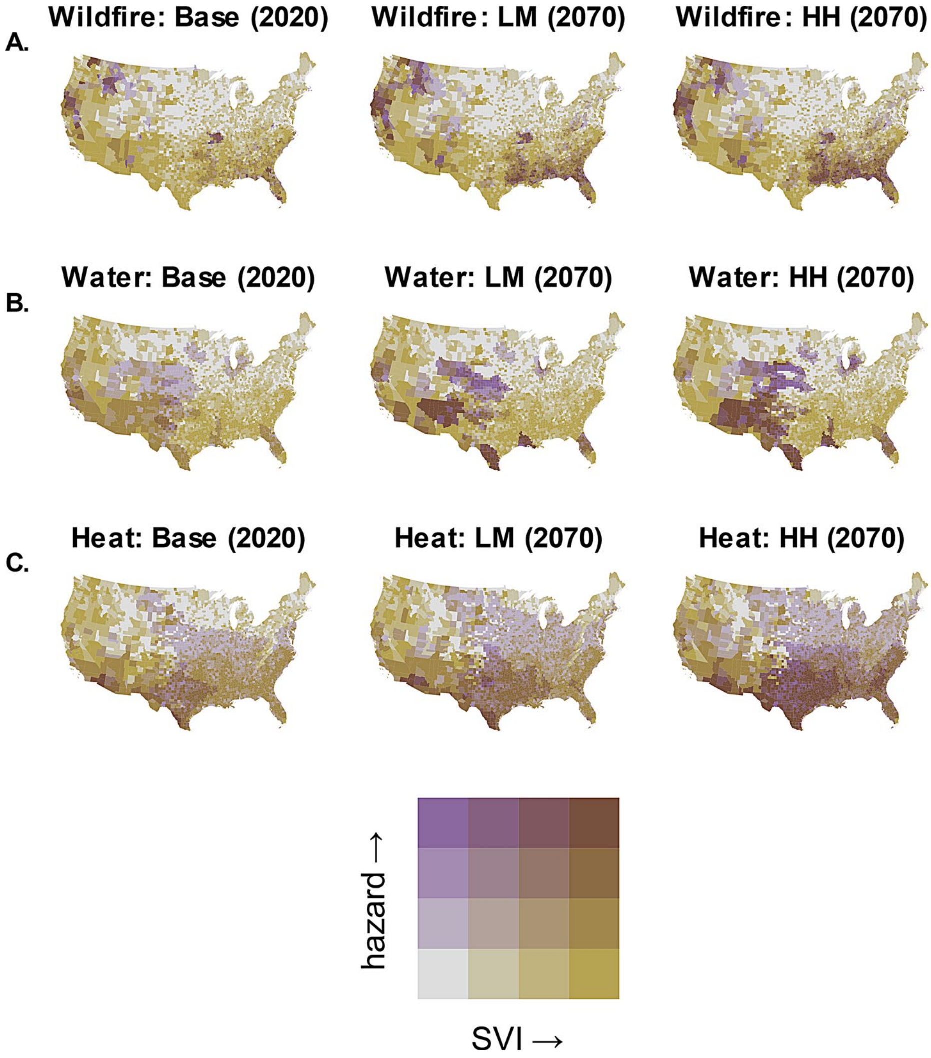

Fig. 9 Bivariate mapping of hazards and the CDC-Social Vulnerability Index (SVI) for: **A**. wildfire, **B**. water shortage, and **C**. heat stress. Columns, from left to right, contain estimates for base period (2020–2030) and for projections to 2070 for scenarios LM and HH. Both SVI and hazard are arrayed into three categories: low, medium-low, medium-high, and high using quartiles for SVI and risk classification schemes described in the methods for hazard risk

northern Idaho) and northeastern Washington. These areas grow and consolidate between 2020 and 2070. In the Southeast wildfire areas of concern grow from a handful of counties in Florida to cover a large area along the lower coastal plain of the Gulf of Mexico—this area expands further to the north under HH.

As with wildfire, areas of concern for water shortage grow in focal areas of the West but also emerge to substantial levels in parts of the East between 2020 and 2070, with areas of both high vulnerability and high exposure emerging in the lower peninsula of Michigan, southern Louisiana, and the northern half of the Florida Peninsula. Areas of concern for heat

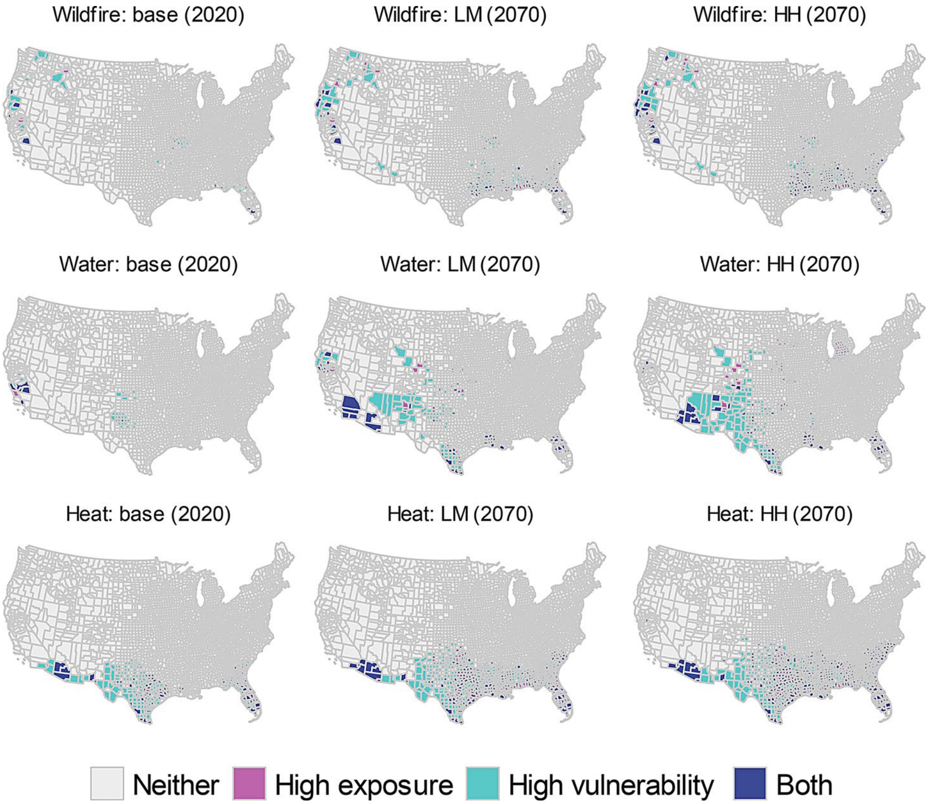

Fig. 10 Areas of concern by hazard defined as areas of medium-high or high hazard assignment that cooccur with high or medium high exposure and/or vulnerability categories (upper quadrants in bivariate classifications in Figs. 8 and 9) for the baseline and two scenarios (LM and HH)

stress grow substantially between 2020 and 2070 throughout the southern tier of the country from Arizona to the Carolinas, with especially high numbers of counties where high vulnerability intersects high exposure.

The intersection of areas of exposure and equity concerns for the three hazards (Fig. 11) shows substantial growth in areas of concern across nearly the entire southern third of the United States from California to Georgia, and in a region that reaches from the high Sierras in central California, into the southern reach of the Cascades in Oregon.

4 Discussion

Our projections show substantial growth in medium high or high-hazard areas for wildfire risk, water shortage, and heat stress between 2020 and 2070, with even greater growth in the total exposure to high hazard levels and in the exposure of populations within vulnerable counties (Fig. 11). These results imply substantial and growing challenges for adaptation efforts.

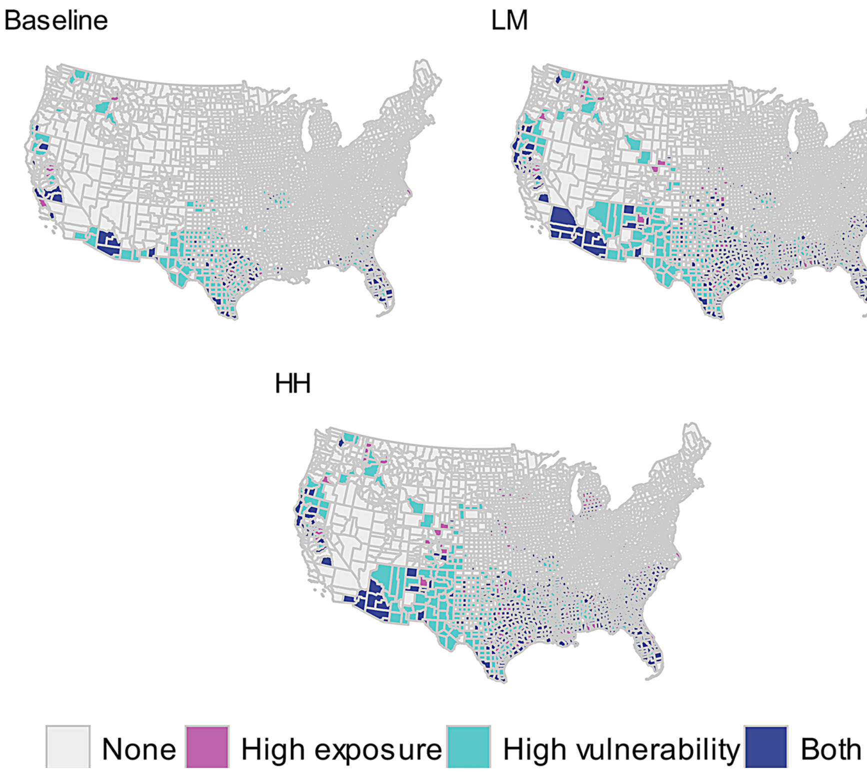

Fig. 11 Areas of concern in counties with a medium threshold assignment (medium-high or high hazard class) for at least one of the hazards in Fig. 10 intersected with medium-high/high exposure or vulnerability class for the baseline and two scenarios (LM and HH)

Across all hazards, the intersection of high hazard with high exposure is relatively small on an areal basis (Fig. 12a)—9–20% for wildfire, 7–15% for water shortage, and 15–30% for heat—and the area where high hazard, high exposure, and high vulnerability overlap is comparably small (1–17%). The patterns are much different when considering the exposure of population rather than area (Fig. 12b). For all hazard categories and scenarios, at least 79% of the population exposed to high hazard is in either a high exposure or high vulnerability county. In the case of water shortage and heat, there is a large overlap between populations in high exposure and vulnerable counties (between 31 and 64% for water shortage and between 34 and 46% for heat), meaning that many counties that are projected to experience high degrees of future water shortage and heat stress are populous counties with high degrees of vulnerability. But for wildfire, high exposure and high vulnerability coincide for only 5–19% of exposed populations across the scenarios so that targeting strategies for wildfire mitigation based on efficiency (targeting areas with largest exposed populations) would greatly differ from those focused on equity (targeting areas with the most vulnerable populations).

These results imply that tradeoffs would arise between managing for efficiency and equity goals in allocating fixed budgets to mitigate harm from wildfire. In contrast, for water shortage and heat, considerable overlap between high exposure and vulnerable counties indicates

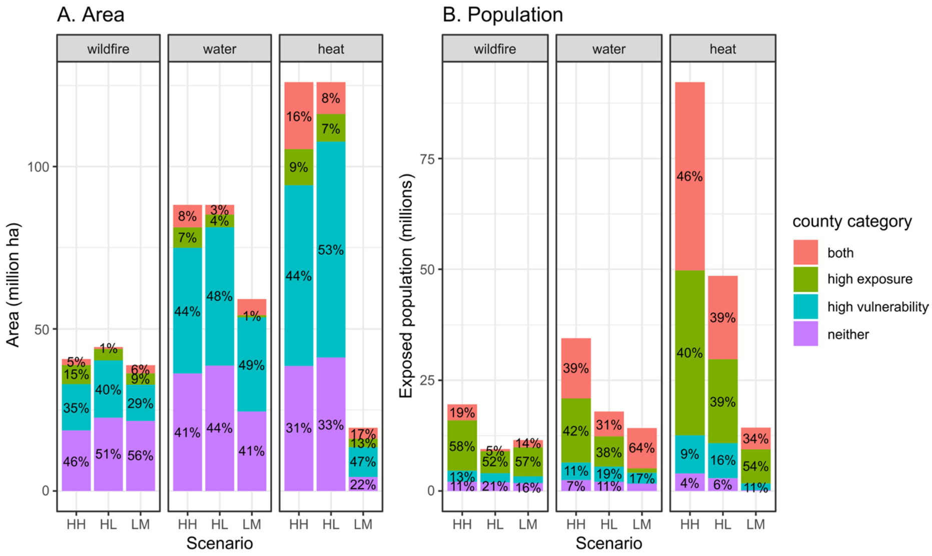

Fig. 12 Area and populations of counties with high hazard risk by exposure and vulnerability classes, with high exposure and high vulnerability defined by the highest quartile of population density and SVI respectively. 'Both' indicates that a county has high population density and high SVI

that targeting high vulnerability counties alone for hazard mitigation would address most exposed populations: 50–81% for water shortage and 45–55% for heat. Resolving differences between efficiency- and equity-based strategies for wildfire management would benefit from more information, especially better measures of how vulnerability amplifies the realized harm to communities. Managers could use these measures (likely imperfect) along with management strategies to deliver public benefits that would support further and generally subjective tradeoff evaluations.

In all three hazard categories, the area of high vulnerability counties experiencing high hazard risk levels is at least an order of magnitude greater than the area of high exposure counties experiencing these risks. The ratio of vulnerable area to high exposure area is 6:1 for wildfire, 11:1 for water shortage, and 20:1 for heat stress, implying that the area needed to be treated to mitigate harm to the most exposed counties is small relative to vulnerable counties—note that these ratios include areas where both exposure and vulnerability are high. Additionally, the most vulnerable counties have populations embedded in much larger landscapes, where effective mitigation may require a much larger treatment area per population protected, generally consistent with US Forest Service emphasis on wildfire treatments in the Wildland-Urban interface in the West (USDA Forest Service 2022).

Results also highlight where hazards might overlap and potentially present compounding effects—consistent with the use of common climate projections across scenarios. Where water shortage and high fire hazard co-occur, we would expect greater consequences from wildfire for municipal watersheds. One case in point is the Front Range of Colorado, where Denver Water has suffered substantial infrastructure losses from large fires in the recent past and is now investing in wildfire mitigation activities.[5] Other areas of potential confluence of water-shortage and wildfire risk include northern California-southern Oregon, large areas

[5] https://www.denverwater.org/tap/keeping-reservoirs-dillon-clean-and-pristine?size=n_21_n.

of Arizona and New Mexico, and southern Louisiana and northern peninsular Florida in the southeast. Where heat stress overlaps with water shortage or wildfire risk, we anticipate compounding implications for human health. In the case of wildfire, heat could reduce the ability of firefighters to effectively suppress fires and workers to mitigate wildfire hazards. In the case of water shortage, the addition of heat stress could compound well-known effects of heat stress on human health and potentially affect the ability to generate electricity in areas with high demands for air conditioning.

Our results indicate that water shortage and heat stress and their intersection with exposure/vulnerability grow in intensity and spread mostly from current areas of concern, but the pattern is different for wildfire. For wildfire we project a major structural change with the emergence of a large area of high hazard–as well as coincidence with high exposure and high vulnerability counties–in the southeast, along the Gulf Coastal Plain. While current US Forest Service wildfire treatment strategies focus on the wildfire crisis in the West, our results indicate perhaps even greater challenges to be found in the Southeast by 2070. Here, landscape ownership patterns are highly variable and dominated by private ownership (> 85%), the characteristics of vulnerable populations is much different (more rural poverty, minority communities, and older populations), and the portion of land cover/use in forests is substantially higher than in the West giving rise to a substantially different policy and management context for hazard mitigation activities.

5 Conclusions

Government agencies face substantial challenges prioritizing investments for widespread risks driven by climate change, including whether to prevent the greatest amount of potential harm (efficiency) or to protect areas where harm per person may be the highest (vulnerability). Such efficiency-vulnerability tradeoffs have no pure analytical solution—that is they require subjective evaluation and difficult choices by decision makers. Efficiency-equity trades have surfaced in many federal and state program areas. For example, housing policy in the US has pursued both broad access to mortgage financing and more equitable access through programs such as Community Development Block Grants for low-income persons. In California, Integrated Regional Water Management funding for improving water infrastructure and future access to water supplies includes grant programs for disadvantaged communities.[6] Our results indicate where high exposure and/or high vulnerability correspond with high hazard. For heat stress and water shortages there is considerable overlap, so prioritizing counties with both high exposure and high vulnerability first would address from 45 to 94% of populations in high exposure areas and 67–87% in high vulnerability areas, but overlap is minimal for wildfire risk.

For wildfire there is little overlap between exposure and vulnerability, amplifying the choice between strategies focused on efficiency and equity criteria. Additionally, the population density of these high vulnerability areas is relatively low, highlighting the challenges and high costs of mitigating harm in the wildland urban interface. The projected changes in wildfire risk would also raise substantial institutional challenges to mitigation activities. The most recent USDA Forest Service wildfire strategy focuses on reducing hazardous fuels as a means to reduce the intensity of future wildfires in the West, where federal lands dominate

[6] https://water.ca.gov/programs/integrated-regional-water-management.

the landscape (USDA Forest Service 2022). In this setting, administrative initiatives can bring fuel treatments and other activities to effective scales in high-hazard areas. Addressing the projected growth in wildfire hazard in the southeast may warrant substantially different policies. Here effective strategies would involve treatment of mostly private forests held by millions of owners—the potential for coordination of treatments across these variable landscapes is much lower, but traditional subsidy/tax treatments may be more effective policy instruments.

Shifting thinking about climate change adaptation and hazard management from disaster response to damage prevention requires knowledge of risk management and the generation of hazard. At the same time, it also requires an understanding of social vulnerability and the interaction of hazard and vulnerability in determining overall human costs. Risk mitigation can involve reducing hazard generation and exposure (i.e., through forest fuel treatments and fuel breaks) but might also directly address factors that determine vulnerability (e.g., infrastructure to improve mobility of elderly and disabled people). Both require understanding the juxtaposition of hazard and vulnerability, what we and others address with coincidence analysis at a broad scale. But effective strategies will depend on site and community specific conditions and interactions that go beyond the scope of our study (e.g., the location of elderly residents, evacuation strategies, access to emergency services).

Many components of our analysis warrant additional study. There is no consensus among the social sciences and practitioners regarding the best measure of vulnerability (Coughlan et al. As described by Tate (2012), appropriate measures of vulnerability vary across types of risks so that vulnerability to wildfire is influenced by factors different from those affecting vulnerability to water scarcity. In addition, across the time horizon of our projections, realized harm could restructure communities and therefore vulnerability (Cremen et al. 2022; Bjarnadottir et al. 2011), in some cases increasing vulnerability over time. Future research would focus on developing dynamic, risk-specific measures of vulnerability. Climate change and realized harm from these and other hazards may also influence the future regional/spatial distribution of populations with different capacities for climate migration across social strata. Our findings indicate future research on the interaction between climate migration and social vulnerability could be especially useful.

We use population density as a proxy for exposure and conduct our risk assessment. More nuanced measures of exposure to fire risk would account for how people, buildings, and other infrastructure are juxtaposed with hazardous fuel loads, for example, as well as for all forms of damage, including smoke impacts on human health. Exposure to water shortage risks would account for water's use within local economies. Useful future research could address more risk-specific measures of exposure.

Future work could further explore the distributional properties of our projections. The selection of scenarios within the framework of the RPA Assessment provides a broad range of projected futures across population, income, and climate variables for this analysis. The scenario variables and resource projections are generated by stochastic models, each with error/variance properties. Here we evaluate the range of outcomes across mean projections for each scenario but recognize that additional insights into variance/error properties would also be informative for applying results to prioritize investments by gauging overall uncertainty but also the robustness of projections by location.

In subsequent research, we might also reconsider the overall structure of this type of analysis. Data and measurement gaps motivate our use of a bivariate categorical analysis following the usual format for spatial risk assessment. This provides a manageable approach to assessing priorities but falls short of explicit quantitative measures of expected damages/harm via hazard probabilities and spatially explicit damage functions. But the use of discrete hazard categories is a first approximation. Given the multiple dimensions of damage and the state of science, complete damage function estimation would require extensive research, but intermediate empirical measures of harm might be within reach.

Supplementary Information The online version contains supplementary material available at https://doi.org/10.1007/s11069-025-07566-9.

Acknowledgments D.N.W. received support from USDA Forest Service Joint Venture Agreement 20-JV-11132650-317, "Linking Policy Analysis to National Resource Assessments."

Authors contribution All authors contributed to the study conception and design. Material preparation, data collection and analysis were performed by David Wear, John Coulson, and Travis Warziniack. The first draft of the manuscript was written by David Wear and all authors commented on previous versions of the manuscript. All authors read and approved the final manuscript.

Funding The authors have no relevant financial or non-financial interests to disclose.

Declarations

Ethical approval The findings and conclusions in this publication are those of the authors and should not be construed to represent any official USDA or U.S. Government determination or policy.

Conflict of interest The authors declare that they have no conflicts of interest.

References

Adams MDO, Charnley S (2018) Environmental justice and US Forest Service hazardous fuels reduction: a spatial method for impact assessment of federal resource management actions. Appl Geography 90 257–271. https://doi.org/10.1016/japgeog201712014

Atkinson AB, Stiglitz JE (1980) Lectures on public economics. McGraw-Hill, New York

Barbero R, Abatzoglou JT, Larkin NK, Kolden CA, Stocks B, Barbero R, Abatzoglou JT, Larkin NK, Kolden CA, Stocks B (2015) Climate change presents increased potential for very large fires in the contiguous United States. Int J Wildland Fire 24 892–899. https://doi.org/10.1071/WF15083

Bjarnadottir S, Li Y, Stewart MG (2011) Social vulnerability index for coastal communities at risk to hurricane hazard and a changing climate. Nat Hazards 59:1055–1075. https://doi.org/10.1007/s11069-011-9817-5

Bouwer LM (2013) Projections of future extreme weather losses under changes in climate and exposure. Risk Anal 33:915–930. https://doi.org/10.1111/j1539-6924201201880x

Brown S, Jenkins K, Goodwin P, Lincke D, Vafeidis AT, Tol RSJ, Jenkins R, Warren R, Nicholls RJ, Jevrejeva S, Arcilla AS, Haigh ID (2021) Global costs of protecting against sea-level rise at 15 to 40°C. Climatic Change 167 4. https://doi.org/10.1007/s10584-021-03130-z

Burke M, Driscoll A, Heft-Neal S, Xue J, Burney J, Wara M (2021) The changing risk and burden of wildfire in the united States. Proc Natl Acad Sci 118(e2011048118). https://doi.org/10.1073/pnas2011048118

Chen K, Vicedo-Cabrera AM, Dubrow R (2020) Projections of ambient temperature- and air pollution-related mortality burden under combined climate change and population aging scenarios: a review. Curr Envir Health Rpt 7 243–255. https://doiorg/ https://doi.org/10.1007/s40572-020-00281-6

Costanza JK, Koch FH, Reeves M, Potter KM, Schleeweis K, Riitters K, Anderson SM, Brooks EB, Coulston JW, Joyce LA, Nepal P, Poulter B, Prestemon JP, Varner JM, Walker DM (2023) Disturbances to forests and rangelands. In: US Department of Agriculture Forest Service. Future of America's Forest and Rangelands: Forest Service 2020 Resources Planning Act Assessment. Gen Tech Rep WO-102. Washington DC. https://doi.org/10.2737/WO-GTR-102-Chap5

Coughlan MR, Ellison A, Cavanaugh A (2019) Social vulnerability and wildfire in the wildland- urban interface. Working Paper no. 96 Ecosystem Workforce Program, Eugene OR. https://www.nwfirescience.org/our-products/social-vulnerability-and-wildfire-wildland-urban-interface

Coulston JW, Brooks EB, Butler BJ, Costanza JK, Walker DM, Domke GM, Caputo J, Markowski-Lindsay M, Sass EM, Walters BF, Guo J (2023a) Forest resources. In: US Department of Agriculture Forest Service. Future of America's Forest and Rangelands: Forest Service 2020 Resources Planning Act Assessment. Gen Tech Rep WO-102 Washington DC. https://doi.org/10.2737/WO-GTR-102-Chap6

Coulston JW, Domke GM, Walker DM, Brooks EB, O'Dea CB (2023b) Near-term investments in forest management support long-term carbon sequestration capacity in forests of the united States. PNAS Nexus 2(11):1–4. https://doi.org/10.1093/pnasnexus/pgad345

Cremen G, Galasso C, McCloskey J (2022) Modelling and quantifying tomorrow's risks from natural hazards. Sci Total Environ 817 152552. https://doi.org/10.1016/jscitotenv2021152552

Crespo Cuaresma J (2017) Income projections for climate change research: a framework based on human capital dynamics. Glob Envir Change 42: 226–236. https://doi.org/10.1016/jgloenvcha201502012

Cutter SL, Finch C (2008) Temporal and spatial changes in social vulnerability to natural hazards. Proc Natl Acad Sci 105:2301–2306. https://doi.org/10.1073/pnas0710375105

Cutter SL, Boruff BJ, Shirley WL (2003) Social vulnerability to environmental hazards: social vulnerability to environmental hazards. Soc Sci Q 84:242–261. https://doi.org/10.1111/1540-62378402002

Drakes O, Tate E (2022) Social vulnerability in a multi-hazard context: a systematic review. Environ Res Lett 17:033001. https://doi.org/10.1088/1748-9326/ac5140

Flanagan BE, Gregory EW, Hallisey EJ, Heitgerd JL Lewis B (2011) A social vulnerability index for disaster management. Journal of Homeland Security and Emergency Management 8. https://doi.org/10.2202/1547-73551792

Flanagan BE, Hallisey EJ, Adams E, Lavery A (2018) Measuring community vulnerability to natural and anthropogenic hazards: the centers for disease control and prevention's social vulnerability index. J Environ Health 80:34–36. https://pmc.ncbi.nlm.nih.gov/articles/PMC7179070/

Gaither CJ, Poudyal NC, Goodrick S, Bowker JM, Malone S, Gan J (2011) Wildland fire risk and social vulnerability in the southeastern united states: an exploratory Spatial data analysis approach. For Pol Econ 13:24–36. https://doi.org/10.1016/jforpol201007009

Heidari H, Arabi M, Warziniack T (2021) Vulnerability to water shortage under current and future water supply-demand conditions across US river basins. Earth's Future 9:e2021EF002278. https://doi.org/10.1029/2021EF002278

IPCC (2022) Global warming of 15°C: IPCC special report on impacts of global warming of 15°C above pre-industrial levels in context of strengthening response to climate change sustainable development and efforts to eradicate poverty. 1st ed Cambridge University Press. https://doi.org/10.1017/9781009157940

Jevrejeva S, Williams J, Vousdoukas MI, Jackson LP (2023) Future sea level rise dominates changes in worst case extreme sea levels along the global coastline by 2100. Environ Res Lett 18(024037) https://doi.org/10.1088/1748-9326/acb504

Joyce LA, Coulson D (2020) Climate scenarios and projections: a technical document supporting the USDA forest service 2020 RPA assessment. Gen tech rep RMRS-GTR-413 fort Collins CO. US Department of Agriculture Forest Service Rocky Mountain Research Station. https://doi.org/102737/RMRS-GTR-413

Langner LL, Joyce LA, Wear DN, Prestemon JP, Coulson D, O'Dea CB (2020) Future scenarios: a technical document supporting the USDA forest service 2020 RPA assessment. Gen Tech Rep RMRS-GTR-412 fort Collins CO: US Department Agric for Service Rocky Mountain Res Stn. https://doi.org/10.2737/RMRS-GTR-412

Modaresi Rad A, Abatzoglou JT, Fleishman E, Mockrin MH, Radeloff VC, Pourmohamad Y, Cattau M, Johnson JM, Higuera P, Nauslar NJ, Sadegh M (2023) Social vulnerability of the people exposed to wildfires in US West Coast States. Sci Adv 9(eadh4615). https://doi.org/10.1126/sciadvadh4615

Mukherjee S, Mishra AK, Mann ME, Raymond C (2021) Anthropogenic warming and population growth may double US heat stress by the late 21st century. Earth's Future 9:e2020EF001886. https://doi.org/10.1029/2020EF001886

O'Dea CB, Langner LL, Joyce LA, Prestemon JP, Wear DN (2023) Future scenarios In: US Department of Agriculture Forest Service 2023 Future of America's Forest and Rangelands: Forest Service 2020 Resources Planning Act Assessment. Gen Tech Rep WO-102 Washington DC https://doi.org/10.2737/WO-GTR-102-Chap3

Riitters K, Coulston JW, Mihiar C, Brooks EB, Greenfield EJ, Nelson MD, Domke GM, Mockrin MH, Lewis DJ, Nowak DJ (2023) Land resources. In: US Department of Agriculture Forest Service 2023 Future of America's Forest and Rangelands: Forest Service 2020 Resources Planning Act Assessment Gen Tech Rep WO-102 Washington DC. https://doi.org/10.2737/WO-GTR-102-Chap4

Saia SM, Suttles KM, Cutts BB, Emanuel RE, Martin KL, Wear DN, Coulston JW, Vose JM (2020) Applying climate change risk management tools to integrate streamflow projections and social vulnerability. Ecosystems 23:67–83. https://doi.org/10.1007/s10021-019-00387-5

Sanchez L, Warziniack T, Knowles M (2023) The inequitable exposure of socially vulnerable groups to water shortage across the conterminous united States. Environ Res Lett 18:044022. https://doi.org/10.1088/1748-9326/acb06d

Schwingshackl C, Sillmann J, Vicedo-Cabrera AM, Sandstad M, Aunan K (2021) Heat stress indicators in CMIP6: estimating future trends and exceedances of impact-relevant thresholds. Earth's Future 9:e2020EF001885. https://doi.org/10.1029/2020EF001885

Spielman SE, Tuccillo J, Folch DC, Schweikert A, Davies R, Wood N, Tate E (2020) Evaluating social vulnerability indicators: criteria and their application to the social vulnerability index. Nat Hazards 100:417–436. https://doi.org/10.1007/s11069-019-

Tate E (2012) Social vulnerability indices: a comparative assessment using uncertainty and sensitivity analysis. Nat Hazards 63:325–347 https://doi.org/10.1007/s11069-012-0152-2

Tilloy A, Malamud BD, Winter H, Joly-Laugel A (2019) A review of quantification methodologies for multi-hazard interrelationships. Earth-Science Rev 196:102881. https://doi.org/10.1016/jearscirev2019102881

USDA Forest Service (2022) Confronting the wildfire crisis: a strategy for protecting communities and improving resilience in America's forests. FS-1187a. Washington, DC: Department of Agriculture, Forest Service, 2022. https://www.fs.usda.gov/managing-land/wildfire-crisis

USDA Forest Service (2023) Future of America's forest and rangelands: forest service 2020 resources planning act assessment. Gen Tech Rep WO -102. U.S. Department of Agriculture, Forest Service, Washington DC. https://doi.org/10.2737/WO-GTR-102

USGCRP (2018) Fourth national climate assessment. US Global Change Research Program Washington DC

Warziniack T, Arabi M, Froemke P, Ghosh R, Heidari H, Rasmussen S, Swartzentruber R (2023) Water resources. In: US Department of Agriculture Forest Service 2023 Future of America's Forest and Rangelands: Forest Service 2020 Resources Planning Act Assessment Gen Tech Rep WO-102 Washington DC. https://doi.org/10.2737/WO-GTR-102-Chap9

Wear DN, Prestemon JP (2019) Spatiotemporal downscaling of global population and income scenarios for the united States. PLoS ONE 14:e0219242. https://doi.org/10.1371/journalpone0219242

Westerling AL, Hidalgo HG, Cayan DR, Swetnam TW (2006) Warming and earlier spring increase western US forest wildfire activity. Science 313:940–943 https://doi.org/10.1126/science1128834

Westfall JA, Coulston JW, Moisen GG, Andersen HE (2022) Sampling and Estimation Documentation for the enhanced forest inventory and analysis program. Gen. Tech. Rep. NRS-GTR-207. U.S. Department of Agriculture, Forest Service, Northern Research Station, Madison, WI. https://doi.org/10.2737/NRS-GTR-207

Yin J, Gentine P, Slater L, Gu L, Pokhrel Y, Hanasaki N, Guo S, Xiong L, Schlenker W (2023) Future socio-ecosystem productivity threatened by compound drought–heatwave events. Nat Sustain 6:259–272. https://doi.org/10.1038/s41893-022-01024-1